Numerical-relativity surrogate modeling with nearly extremal black-hole spins

OPEN ACCESS
IOP Publishing
Classical and Quantum Gravity
Class. Quantum Grav. **40** (2023) 055003 (15pp) https://doi.org/10.1088/1361-6382/acb3a7

Numerical-relativity surrogate modeling with nearly extremal black-hole spins

Marissa Walker[1,*], **Vijay Varma**[2,5], **Geoffrey Lovelace**[3] and **Mark A Scheel**[4]

[1] Christopher Newport University, Newport News, VA 23606, United States of America
[2] Max Planck Institute for Gravitational Physics (Albert Einstein Institute), D-14476 Potsdam, Germany
[3] Nicholas and Lee Begovich Center for Gravitational Wave Physics and Astronomy, California State University Fullerton, Fullerton, CA 92834, United States of America
[4] Theoretical Astrophysics, Walter Burke Institute for Theoretical Physics, California Institute of Technology, Pasadena, CA 91125, United States of America

E-mail: marissa.walker@ligo.org

Received 4 August 2022; revised 14 December 2022
Accepted for publication 16 January 2023
Published 2 February 2023

Abstract

Numerical relativity (NR) simulations of binary black hole (BBH) systems provide the most accurate gravitational wave predictions, but at a high computational cost—especially when the black holes have nearly extremal spins (i.e. spins near the theoretical upper limit) or very unequal masses. Recently, the technique of reduced order modeling has enabled the construction of 'surrogate models' trained on an existing set of NR waveforms. Surrogate models enable the rapid computation of the gravitational waves emitted by BBHs. Typically these models are used for interpolation to compute gravitational waveforms for BBHs with mass ratios and spins within the bounds of the training set. Because simulations with nearly extremal spins are so technically challenging, surrogate models almost always rely on training sets with only moderate spins. In this paper, we explore how well surrogate models can extrapolate to nearly extremal spins when the training set only includes moderate spins. For simplicity, we focus on one-dimensional surrogate models trained on NR simulations of BBHs with equal masses and equal, aligned spins. We

[5] Marie Curie Fellow.
[*] Author to whom any correspondence should be addressed.

assess the performance of the surrogate models at higher spin magnitudes by calculating the mismatches between extrapolated surrogate model waveforms and NR waveforms, by calculating the differences between extrapolated and NR measurements of the remnant black-hole mass, and by testing how the surrogate model improves as the training set extends to higher spins. We find that while extrapolation in this one-dimensional case is viable for current detector sensitivities, surrogate models for next-generation detectors should use training sets that extend to nearly extremal spins.

Keywords: gravitational waves, surrogate modeling, high spin black holes

(Some figures may appear in colour only in the online journal)

1. Introduction

Since the first detection of gravitational waves by the Laser Interferometer Gravitational-Wave Observatory (LIGO) in 2015 [1], Advanced LIGO [2] and Virgo [3] have observed dozens of gravitational waves from merging black holes as the waves passed through Earth [1, 4–6]. As gravitational-wave detectors' sensitivities continue to improve, they will detect many more [7].

The observed gravitational-wave signals encode a wealth of information about each source's nature and behavior. But extracting this information ('parameter estimation') is a computationally intensive process of comparing many model waveforms with the data; appendix E of [6], e.g. summarizes state-of-the-art parameter estimation techniques.

Binary black holes (BBHs) emit gravitational waves as the black holes spiral together, merge into a new, larger remnant black hole that rings down into equilibrium. Long before the time of merger ('inspiral') and after the time of merger ('ringdown'), approximate analytical approaches can give accurate models of the gravitational waves; however, near the time of merger, all analytic approximations fail; the waveforms can only be computed using numerical relativity (NR). (For a recent review of NR techniques for modeling merging black holes, see, e.g. [8].)

Developing high-accuracy waveform models will be especially important as detectors improve their sensitivity, as signals will be recovered with higher signal-to-noise ratios(SNRs). Studies of the performance of current waveform models with predicted third generation detector sensitivities show that there needs to be an improvement of semi-analytic models' accuracy by three orders of magnitude, and an improvement of NR accuracy by one order of magnitude [9]. NR calculations are the most accurate way to compute the gravitational waves emitted by merging black holes, but they are too computationally expensive to feasibly yield the large number of waveforms that gravitational-wave inference methods require. One approach to overcoming this challenge is the construction of approximate, semi-analytic models [10–17] that are calibrated to and validated against catalogs of NR waveforms. For instance, two such models, SEOBNRv4PHM [10] and IMRPhenomXPHM [11], were used to infer the properties of BBHs in the most recent Gravitational-Wave Transient Catalog [6].

An alternative approach is to create a stand-in, or 'surrogate,' model [18] that effectively interpolates an existing set of NR waveforms (the 'training set'), each with different binary parameters, to produce a waveform with a desired set of binary parameters. After a surrogate model is created, it can quickly evaluate a gravitational waveform whose parameters are contained within the most extreme parameters of the training set. Surrogate models can also extrapolate beyond their training set, but the results become progressively less accurate. Surrogate models trained directly on NR simulations [19–21] have been used alongside

approximate, semi-analytic models in recent analyses of LIGO-Virgo gravitational wave observations [5, 22–29]. Surrogate models have an advantage in accuracy over approximate, semi-analytic models when comparing with NR, but they also have some disadvantages: they are only guaranteed to be accurate within the parameter space spanned by the training set, and their length (i.e. number of orbits) is limited to the length of the training waveforms, meaning they can only span a detector's sensitive frequency band for binaries with sufficiently high masses (although, this limitation has been lifted for aligned-spin BBHs [20]).

One particularly interesting region of BBH parameter space is binaries containing a black hole spinning nearly as rapidly as theoretically possible; observational evidence (e.g. [30]) suggests that such black holes exist and thus might be among the merging black holes that gravitational-wave detectors will observe. Black hole spins are described in this paper using the dimensionless spin $\chi = S/M^2$ (where S is the spin angular momentum and M is the Christodoulou mass of the black hole), which ranges from -1 to 1, with the most rapidly spinning black holes having spins close to ± 1. Current surrogate models based on NR [19–21] are typically trained on waveforms containing black holes with spins up to $\chi = 0.8$. This limitation follows from the practical difficulty in modeling merging black holes with nearly extremal spins [31, 32].

Ideally, waveform models would cover the entire parameter space, but creating a training set of high spin and high mass ratio waveforms is computationally challenging and expensive. Using current surrogate models to predict BBH waveforms including a rapidly spinning (greater than 0.8) black hole requires extrapolation beyond the training parameters in spin. This work explores two questions within the context of a simplified one-dimensional surrogate model: the accuracy of such extrapolation compared with NR, and the potential for improving high spin models by expanding the training set.

The rest of this paper is organized as follows: section 2 describes the methods used for constructing surrogate models, summarizes the process of producing the NR waveforms that were used, and estimates the level of accuracy needed for waveforms. Section 3.2 presents the one-dimensional waveform surrogate models and analysis of results for extrapolation to high spin. Section 3.4 presents the results of using the same surrogate modeling process to predict the mass and spin of the remnant black hole. Section 4 summarizes the findings and future outlook of the work. Note that throughout this paper we use units $G = c = 1$.

2. Methods

2.1. Surrogate modeling

Surrogate models trained on NR waveforms are a fast way of constructing the many waveforms needed for parameter estimation. Several NR surrogate waveform models exist covering various ranges of parameters. Generically, BBHs can be described using seven dimensions: three dimensions to describe the spin of each black hole, and one to describe the mass ratio between the two black holes ($q = M_1/M_2$, where we choose the convention that M_1 is the heavier object, so $q \geqslant 1$). Two existing surrogate models will be used to show the capabilities of current models for high spin black holes. One model is the NRSur7dq2 surrogate model, which covers generically spinning black holes (including precession following from spins misaligned with the orbital angular momentum) with mass ratios up to 2 and spin magnitudes $\chi_{1,2} \leqslant 0.8$ [21]. A recent update to this model, NRSur7dq4 [19], expands the mass ratio range to 4, but results in this paper use NRSur7dq2 since here we treat only the equal-mass case. Another model NRHybSur3dq8 [20], includes mass ratios

up to 8, but only for non-precessing spins. This three dimensional model is also hybridized with analytic models to create waveforms longer than the NR simulations by combining the early inspiral from analytic models with the final portion near and after the time of merger from NR.

The surrogates produced in this paper use a similar method to those previous models, as described in [20]. The initial step in the process is gathering the NR waveforms of the training set from the SXS Catalog (section 2.2). The waveforms were chosen to span the desired parameter space, and to take advantage of waveforms that already exist in the catalog. Specifically, we used waveforms where the two black holes had equal mass (mass ratio $q = 1.0$) and equal, aligned or anti-aligned spin. Different ranges of spin were used for different surrogates, as described in section 3.

The waveforms are time-shifted such that the peak of the signal occurs at time $t = 0$, and the beginning of the waves are truncated such that all the waveforms begin at the same time and do not include the initial burst of spurious gravitational waves at the beginning of each simulation (these spurious waves are caused by limitations in the methods used to construct initial data). The surrogates presented in this paper use an initial time of -1000 M, at which time the frame is aligned so that the initial orbital phase is zero. The number of orbits before merger included in this amount of time depends on the spin of the black holes and is listed for each case in table 1. For the surrogates presented in this paper, since all of the BBHs have mass ratio $q = 1$ and have spin that is aligned or anti-aligned with the orbital axis, the $l = m = 2$ spin-weighted spherical harmonic modes of gravitational radiation will dominate (for details on the importance of the other modes, see [33–36]). For this reason, we have only included the $l = m = 2$ mode. This is a simplification in order to take a first step towards exploring the effects of surrogate modeling in the high spin parameter space in the equal mass systems, but future models used for analysis would be expanded to include other modes (for example, see [20]). Surrogate models work better when the training data consists of slowly varying functions, so the training waveforms are decomposed into separate data pieces that are more slowly varying in time. In this case, the data pieces used are the amplitude and phase of the (2,2) mode of the waveform. For each data piece a separate surrogate is constructed, and then the final waveform is modeled by combining the different data pieces.

2.1.1. Surrogate construction. Given the waveform data pieces, we build a surrogate model for each data piece using the same procedure as section V.C of [20], which we summarize below.

For each waveform data piece, we first construct a linear basis using the greedy basis method [37], with tolerances of 10^{-2} radians for the phase data piece and 10^{-3} for the amplitude data piece of the (2,2) mode. Next, we construct an empirical time interpolant [38] with the same number of empirical time nodes as basis functions for that data piece. Finally, for each empirical time node, we construct a parametric fit for the waveform data piece. For the surrogates created here, the only varying parameter is the spin of the black holes. Since each black hole pair has equal spins ($\chi_1 = \chi_2$), the surrogates are one-dimensional, and the fit parameter is the spin. The fits are constructed using the forward-stepwise greedy parametric fitting method described in appendix A of [39] allowing up to fourth order monomials in the basis functions. To avoid overfitting, a cross-validation step is taken where ten trial fits are performed, leaving out one waveform in each one to validate the fit.

In addition to waveform surrogates, we also created surrogates to interpolate the final mass and spin of the remnant black hole as a function of the initial spin. We followed the approach of [19, 40] but ignored the recoil velocity because it is zero due to the symmetries of equal mass, equal spin BBHs.

2.2. NR waveforms

We train our surrogate models using previously published NR waveforms from the Simulating eXtreme Spacetimes (SXS) catalog [41, 42]. Here, we briefly summarize the techniques that Spectral Einstein Code (SpEC) uses to simulate BBHs; for a recent, more detailed discussion of these techniques, see section II of [42] and the references therein.

Each waveform was computed using the SpEC [43]. SpEC constructs BBH initial data in quasi-equilibrium by solving the eXtended Conformal Thin Sandwich formulation of the Einstein constraint equations [44, 45] using excision boundary conditions [46] and free data based on a weighted superposition of two Kerr–Schild black holes [47]. SpEC then evolves the initial data by solving the generalized-harmonic formulation of the Einstein evolution equations [48] using a pseudospectral approach [49] with a constraint-preserving boundary condition applied on the outer boundary [50].

The singularities are excised from the computational domain, with a control system dynamically transforming the computational grid to conform to the black holes' apparent horizons as they move and deform while ensuring that the excision boundaries require no boundary condition (by ensuring that the characteristic speeds are all outgoing) [51, 52]. When the black-hole spins are nearly extremal, the excision problem becomes especially delicate: as the spin approaches the theoretical maximum, the excision surface must conform more and more precisely to the apparent horizon—while remaining inside of it—to avoid incoming characteristic speeds. Recent improvements in SpEC's techniques [31] have enabled SpEC to simulated BBHs with spins near the theoretical maximum. Specifically, SpEC has simulated merging black holes with dimensionless spin χ as high as 0.998 [42].

2.3. Surrogate accuracy

The surrogate models must be sufficiently accurate—but how accurate is accurate enough? Ensuring that current and future gravitational wave detectors can precisely determine the physical properties of the loudest black hole mergers that they observe and can precisely compare the waves with general relativity's predictions [53] require model waveforms whose numerical errors do not exceed the experimental uncertainty. As an observed gravitational wave's SNR increases, the theoretical models must become correspondingly more accurate.

One way to measure the error in a waveform is the *mismatch* between the waveform and a fiducial waveform. The mismatch between two complex waveforms h_1 and h_2 is calculated in the time domain, using:

$$\mathcal{M} = 1 - \frac{\langle h_1, h_2\rangle}{\sqrt{\langle h_1, h_1\rangle \langle h_2, h_2\rangle}}, \tag{1}$$

where the inner product between waveforms is defined by

$$\langle h_1, h_2\rangle = \left| \int_{t_{\rm min}}^{t_{max}} h_1(t) h_2^*(t) dt \right|. \tag{2}$$

The mismatch is analogous to taking one minus the dot product between two unit vectors. If the vectors (waveforms) are identical, the mismatch will be zero. Note that this mismatch calculation is performed without any assumption of a specific detector's noise curve. We use a flat noise curve because we are trying to understand the limitations of the model itself, rather than testing it within a particular noise realization. Although the results presented here should generalize to different detectors' noise curves, a more detector-specific analysis could be a subject of future study.

As a crude estimate, two template waveforms may be considered to be indistinguishable if mismatch between them is low enough that the following condition is met [54]:

$$\mathcal{M} < \frac{\mathcal{D}}{2\rho^2} \tag{3}$$

where $\mathcal{M}$ is the mismatch between the two waveforms, $\mathcal{D}$ is the number of parameters used to describe the detection (which is 8 for generically spinning black holes assuming circular orbits), and ρ is the SNR of the detection. Therefore as SNRs increase, the acceptable level of error in the theoretical waveforms decreases. As an example, in the first three observing runs of the current detectors, the loudest gravitational wave signal from a BBH system was GW200129_065458, with SNR of 26.5 combined between three detectors [6]. Using the mismatch condition above, a mismatch of $\mathcal{M} < 5.7 \times 10^{-3}$ would be sufficient. However, if an optimally oriented BBH signal with the same properties and distance as the first BBH detection, GW150914, were to happen when LIGO reaches its design sensitivity, the SNR could be nearly 100 for a single detector [55], corresponding to a required mismatch of 4×10^{-4}.

BBH observations could be detected with SNR up to several hundred or even 1000 with third-generation detectors [56, 57]. With an SNR of 1000, the mismatch condition goes down to $\mathcal{M} < 4 \times 10^{-6}$. It is therefore critical to push the boundaries of accuracy in waveform modeling, as well as the models' efficiency to produce large numbers of waveforms for parameter estimation.

3. Surrogate modeling for high spin

We used existing NR waveforms from the SXS catalog [42] to create and test one-dimensional surrogate models, first to examine the effects of extrapolation beyond current surrogate spin levels and then to test the extrapolation with different training sets. All surrogate models used in these tests follow a similar method to that described in [20].

3.1. Case numbers and information about waveforms

All of the waveforms used in the training and validation sets for the one-dimensional surrogate models presented in this paper are publicly available in the SXS Waveform Catalog. Table 1 summarizes the configurations used. All of these waveforms are BBH systems with equal masses, and equal spins either aligned or anti-aligned with the orbital angular momentum. Each binary has initial parameters tuned [58] so that the initial orbital eccentricity at most of order 10^{-3}. Before training or testing the surrogates, all of these waveforms were cropped to an initial time of -1000 M before the merger and a final time of 75 M after the merger.

3.2. Extrapolation beyond training set

First to determine the applicability of current surrogate models to the high spin parameter space, existing models can be extrapolated beyond their optimal (training set) range to create waveforms for rapidly spinning BBHs. Several different parameters were chosen for this prediction based on existing numerical simulations within the SXS catalog, so that mismatch comparisons could show how accurate this extrapolation is. Specifically, we chose test cases that have equal aligned spin and equal mass, so the only parameter that varies is the magnitude of the spin. The top plot in figure 1 demonstrates the capability of two existing models to accurately model systems within the parameter space of their training set, as well as the effects of extrapolating beyond the training set range.

Table 1. The numerical-relativity waveforms used in the surrogate models and testing shown in this paper. Each simulation models merging binary black holes with equal masses ($q = 1.000$) and equal spins aligned or anti-aligned with the orbital angular momentum. Shown are the simulation name, the spin of each black hole, an estimate of the orbital eccentricity, the number of orbits $N_{\rm orbits}$ simulated before merger, and the number of orbits before merger actually used in the analysis in this paper (corresponding to the time 1000M before merger).

Name	χ_{1z}	χ_{2z}	e	$N_{\rm orbits}$ in simulation	$N_{\rm orbits}$ used
SXS:BBH:0180	-3.7×10^{-9}	-2.16×10^{-9}	5.110×10^{-5}	28.18	6.45
SXS:BBH:0149	−0.2000	−0.2000	1.604×10^{-4}	17.12	6.16
SXS:BBH:0150	0.2000	0.2000	2.714×10^{-4}	19.82	6.76
SXS:BBH:0148	−0.4376	−0.4376	$<3.5 \times 10^{-5}$	15.45	5.85
SXS:BBH:1122	0.4376	0.4376	3.727×10^{-4}	21.53	7.17
SXS:BBH:0151	−0.5999	−0.5999	$<4.8 \times 10^{-4}$	14.48	5.65
SXS:BBH:0152	0.6000	0.6000	4.272×10^{-4}	22.64	7.46
SXS:BBH:0154	−0.7998	−0.7998	$<6.4 \times 10^{-4}$	13.24	5.42
SXS:BBH:0155	0.7999	0.7999	5.051×10^{-4}	24.09	7.86
SXS:BBH:0153	0.8498	0.8498	8.694×10^{-4}	24.49	7.96
SXS:BBH:0159	−0.8996	−0.8996	$<8.1 \times 10^{-4}$	12.67	5.31
SXS:BBH:0160	0.8997	0.8997	4.442×10^{-4}	24.83	8.06
SXS:BBH:0156	−0.9490	−0.9490	7.671×10^{-4}	12.42	5.26
SXS:BBH:0157	0.9496	0.9496	1.483×10^{-4}	25.15	8.17
SXS:BBH:1137	−0.9692	−0.9692	4.313×10^{-4}	12.19	5.24
SXS:BBH:0172	0.9794	0.9794	1.128×10^{-3}	25.35	8.23
SXS:BBH:0177	0.9893	0.9893	$< 2.00 \times 10^{-3}$	25.40	8.25
SXS:BBH:1124	0.998	0.998	8.70×10^{-4}	25.73	8.27

As might be expected, as the models are extrapolated further beyond the training set range, the mismatches with NR simulations get worse. In fact, the rapid increase in mismatch outside of the training set range appears to be almost exponential (although the exact nature of this relationship is not known, and determining it is beyond the scope of this work). However, even the highest spin case shown ($\chi = 0.9893$) is still predicted with a mismatch of less than the mismatch criteria for current detectors. While this result is promising for the applicability of current surrogate models across the entire spin parameter space (at least in the equal mass and equal, aligned spin case), improvements in the models are needed to meet the mismatch criteria for future detectors.

Next, to create a simplified model solely for the purposes of exploring the effects of spin, a one-dimensional surrogate model was created from a set of waveforms with equal mass and equal, aligned spin. Specifically, the waveforms used were the first nine in table 1 with spin $\chi \leqslant \pm 0.8$. The lower plot in figure 1 shows the mismatches between the NR simulations and the evaluations of this simplified surrogate model. Since the test cases with $\chi \leqslant \pm 0.8$ were also part of the training set used to create the model, the mismatches for those cases are also shown with a 'leave one out test', where the model was recreated by leaving out only that test case from the training set and then doing the mismatch test on that case. These tests showed that this simplified model is roughly comparable or a bit better than existing models, so we can use this technique to explore different types of training sets.

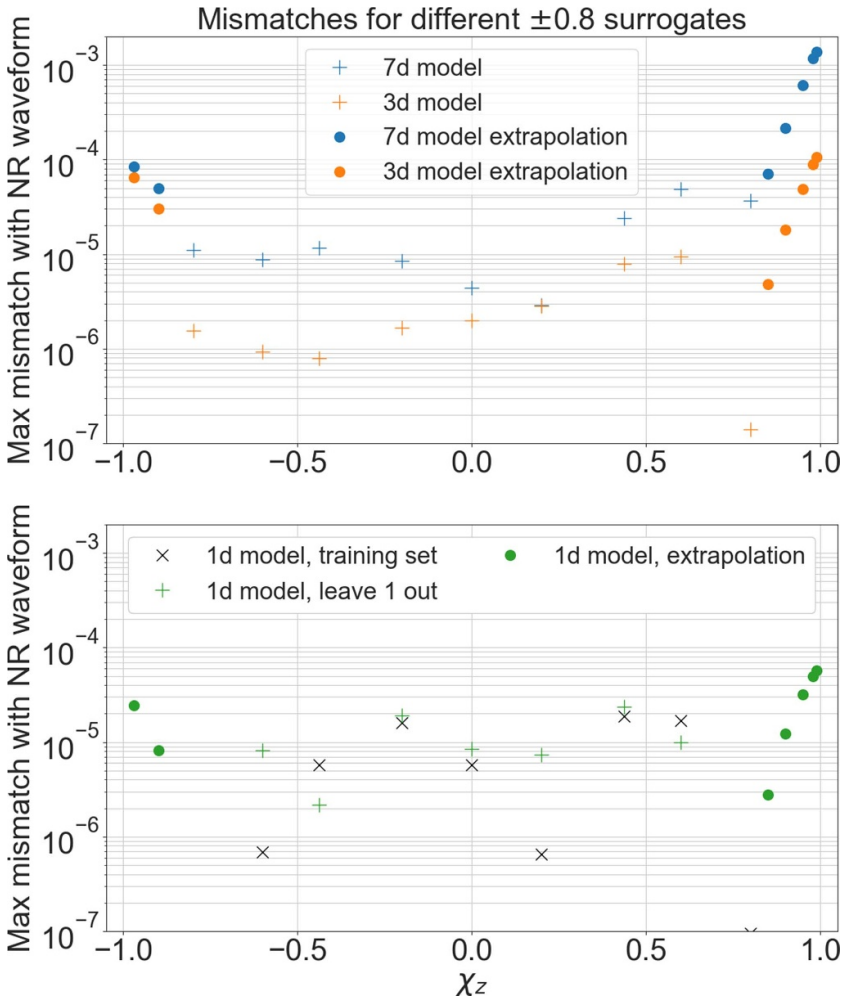

Figure 1. Above: Mismatches between numerical relativity and surrogate evaluation for various spins for a set of equal mass, equal and aligned spin black holes, using two existing surrogate models, NRSur7dq2 and NRHybSur3dq8, using test cases from the NR waveforms listed in table 1. Below: Mismatches between the NR simulation and surrogate evaluation using a one-dimensional surrogate model in spin. The surrogate model was trained on nine simulations of equal mass and equal aligned spin, with spins from -0.8 to 0.8. A leave-one-out validation study was also performed, with surrogate models trained on the same set except for one of the waveforms. For the validation cases, the corner case waveforms (spin -0.8 and 0.8) were left in the model each time. In all cases in both plots, models were trained spin magnitudes up to 0.8. As the models are used to extrapolate farther from that training set range, the mismatches get worse.

3.3. Varying the spin in the training sets

We then created several different one-dimensional surrogate models, each with a different number of training set waveforms that include a different range of spins. Each training set used a subset of the waveforms listed in table 1. These sets were created by choosing all of the cases within the range of spins from $\pm|\chi_{\rm max}|$, where the maximum spin $\chi_{\rm max}$ was different

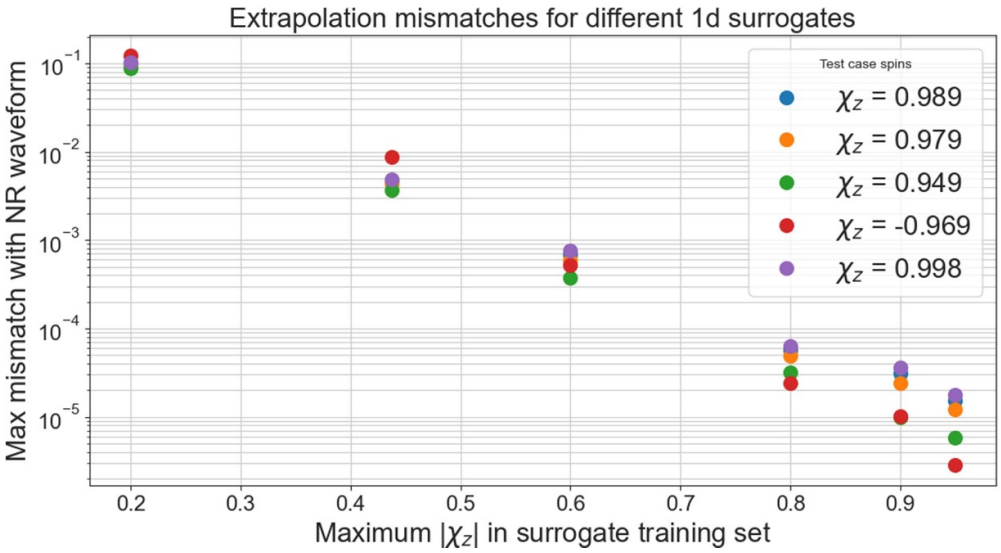

Figure 2. Mismatches with NR simulations and surrogate evaluation of five high spin test cases, for surrogates with different training sets. Each training set encompasses a range of spins from $\pm|\chi_z|$. As the maximum spin included in the training set increases, the extrapolation mismatch gets smaller. (Note that for the 0.95 spin case, the waveform was a validation case as well as a training case for the surrogate with maximum spin of 0.95.)

for each training set. For example, the training set for the $|\chi_{\rm max}| = 0.2$ model simply consisted of the first three cases in the table, with spins of 0 and ± 0.2. The next model created (with $|\chi_{\rm max}| = 0.4376$) was trained on the first five cases, including the original three plus the two higher spin cases. Each set therefore contained two additional training cases from the previous set.

For each different training set, we tested how well the model extrapolated to the most rapidly spinning black holes. Specifically, we used spins of magnitude 0.949 and greater to test the extrapolation of the models. Figure 2 shows the mismatch test results from these different surrogates. As expected, when only using three low spin waveforms up to maximum spin magnitude of 0.2, the model has huge errors when extrapolating to high spin. With each additional set of corner points added, however, the mismatches decrease. Even only including up to 0.6 spins in the training sets reduces the extrapolation mismatches for all of the validation cases to less than 1×10^{-3}. Two of the surrogates tested and shown in figure 2 have an expanded training set beyond $|\chi| = \pm 0.8$: one includes up to $|\chi| = \pm 0.9$, and the other up to $|\chi| = \pm 0.95$. We see that the trend continues, with these surrogates trained on higher spin performing better in their predictions of the high spin waveforms.

In the tests shown in figure 2, the number of waveforms in the training set changed with each different surrogate, as well as the maximum spin. In order to isolate the effect of the spin in the training set, we repeated the procedure of creating multiple surrogates with different maximum spins but the same number of waveforms in each training set. First, we created multiple surrogates with only three waveforms in each training set: 0 and $|\pm\chi_{\rm max}|$, where the maximum spin changed each time. When these surrogates are extrapolated to evaluate the highest spin waveforms, there is still a clear effect of lower mismatches when the maximum

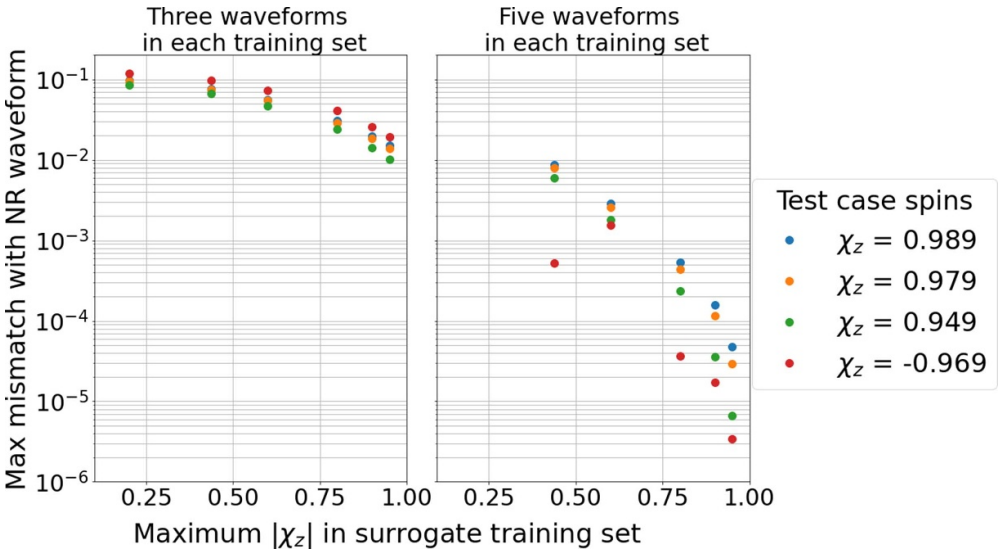

Figure 3. Both plots above show the results of extrapolating to high spin waveforms using surrogates trained on different sets, similar to figure 2. However, in these cases, the number of waveforms is fixed, and only the maximum spins change. In the plot on the left, each training set consists of only three waveforms: 0 and $\pm|\chi_{\rm max}|$. With only three points in the training set, the mismatches are all fairly high, even when $|\chi_{\rm max}|$ is 0.95. However, there is an improvement as the spin increases. On the right hand side, each training set consists of five waveforms: 0, $\pm$0.2, and $\pm|\chi_{\rm max}|$. While the mismatches are still not quite as good as when the training set size increased at every step, there is a significant improvement with increasing the maximum spin in the training set.

spin is increased. However, the mismatches are all significantly higher, with the lowest mismatches being about 10^{-2}. Next, we used five waveforms in each training set: 0, $\pm$0.2, and $\pm|\chi_{\rm max}|$. In these cases, the mismatches are significantly lower, though not quite as low as the surrogates where all the possible waveforms between $\pm|\chi_{\rm max}|$ were used. The mismatch results from these tests are shown in figure 3.

3.4. Remnant mass surrogate models

A similar process can be followed to develop a model not for the full predicted gravitational waveform, but simply for the properties of the remnant black hole, specifically the mass and spin of the remnant.

Just as described above, we first trained a remnant surrogate on the nine BBHs in table 1 with spin magnitudes less than or equal to 0.8, using the same surrogate model fitting procedure as for the waveform model. To test the capabilities of this surrogate within the realm of the training set, we performed leave-one-out tests as described above. Then we tested the surrogate model's ability to extrapolate to high spin. As a reference, the NRSur7dq4Remnant surrogate model (described in [19]) was also evaluated at the same points. The surrogate model errors, or the differences in the surrogate predictions from the NR calculations, both for the interpolated and extrapolated cases, are shown in figure 4. Similar to the waveform surrogate models, most

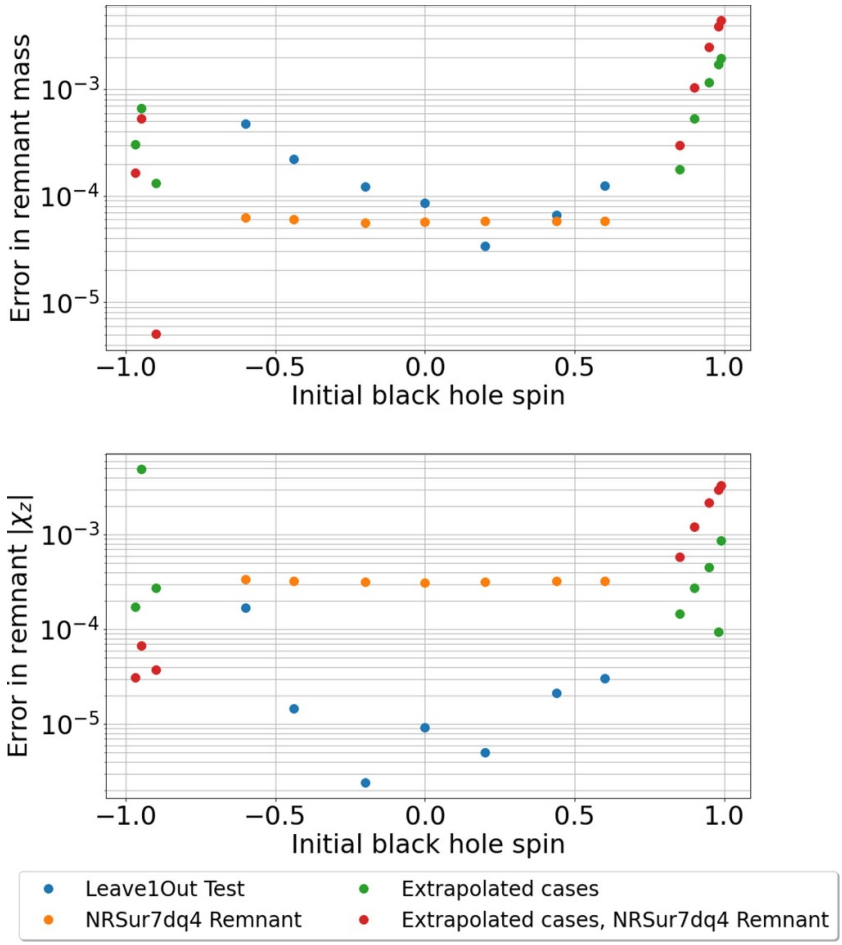

Figure 4. Differences between the remnant masses and spins computed from the NR simulations in table 1, and the remnant masses and spins computed by two remnant surrogate models. Blue: Leave-one-out tests with the 1D surrogate, where that particular waveform was left out of the training set and used only for testing. Orange: Cases from the table with spins $|\chi| \leqslant 0.8$ compared to the surrogate model NRSur7dq4Remnant. Green: Extrapolated predictions with the 1d model. Red: Extrapolated predictions from the NRSur7dq4Remnant model.

of the extrapolated cases have a higher error than those within the training set range, with errors increasing as the extrapolation gets further away from the training range.

Similar to the waveform surrogates, we prepared several different one-dimensional surrogates trained on different ranges of spin and tested how well each of these performed on extrapolating to extreme spin cases. The differences between these predictions and the NR calculations are shown in figure 5. In these surrogates, all of the waveforms from table 1 between $\pm|\chi_{\rm max}|$ were used for each training set. Once again, the trend matches what that of the waveform surrogate studies: expanding the training set to include the higher spin BBHs improves the extrapolation to high spin.

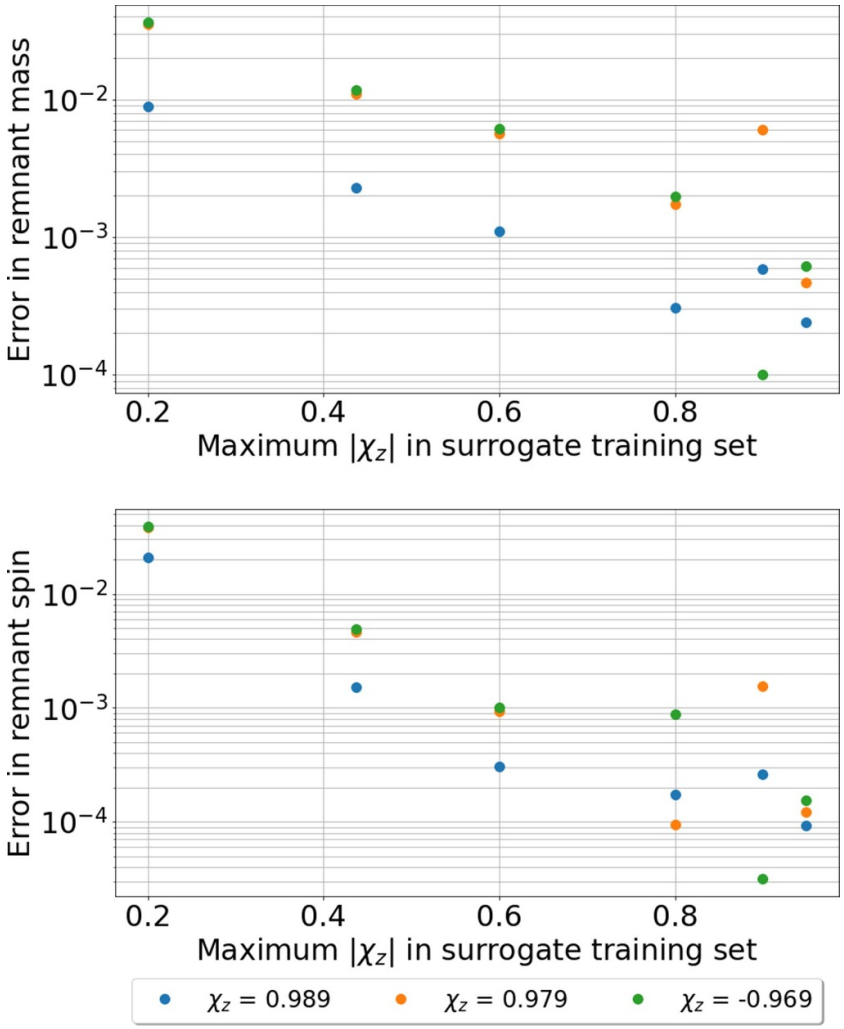

Figure 5. Surrogate model errors (differences from NR calculations) in the extrapolated remnant mass and spin predicted by different one-dimensional surrogate models trained with different training sets with different maximum spins. Similar to the waveform surrogate, there is a clear overall pattern of decreasing error as the training set is expanded to include higher spin simulations.

4. Conclusions

One main conclusion from this study is that extrapolation from surrogate models might actually be viable to some extent for current detector sensitivities. There are of course limitations in the study, since we were only extrapolating in one dimension. Additionally, higher order modes beyond the $l = m = 2$ mode have not been considered. Further study would need to be conducted to test extrapolation in a more generic case; for example a BBH with unequal masses. However, it is promising that for the simplest cases shown here, mismatches for extrapolating to rapid spins may already be suitable for the SNRs expected to be detected from current detectors, and possibly even for future detectors. This finding is consistent with tests

of the surrogate model NRSur7dq4, which was trained on mass ratios up to 4 but was shown to produce accurate predictions of BBHs up to mass ratios of 6 [19].

To reach mismatches of the order of 10^{-6} (which is sufficient for indistinguishability for SNR 1000 observations) across the parameter space, however, the models would need to be improved. This study shows that surrogate extrapolation in spin will continue to improve if we include higher spin waveforms in training sets. When we have higher signal-to-noise observations we will want more accurate models and expanded parameter space. Therefore it is worthwhile to continue to conduct high spin simulations, especially with unequal masses, in order to expand the applicability of surrogate models. Advances in numerical relativity simulations as well as surrogate modeling methods remain important for progressing towards this increased level of accuracy.

Data availability statement

The data that support the findings of this study are available upon reasonable request from the authors.

Acknowledgments

This work was supported in part by NSF award PHY-2011975 at Christopher Newport University; by NSF awards PHY-1654359 and PHY-1606522 and by the Dan Black Family Trust and Nicholas and Lee Begovich at Cal State Fullerton. V V acknowledges funding from the European Union's Horizon 2020 research and innovation program under the Marie Skłodowska-Curie Grant Agreement No. 896869. M S acknowledges funding from the Sherman Fairchild Foundation and by NSF Grant Nos. PHY-2011961, PHY-2011968, and OAC-1931266 at Caltech.

ORCID iDs

Marissa Walker https://orcid.org/0000-0002-7176-6914
Vijay Varma https://orcid.org/0000-0002-9994-1761
Geoffrey Lovelace https://orcid.org/0000-0002-7084-1070
Mark A Scheel https://orcid.org/0000-0001-6656-9134

References

[1] Abbott B P *et al* (LIGO Scientific Collaboration and Virgo Collaboration) 2016 *Phys. Rev. Lett.* **116** 061102
[2] Aasi J *et al* (LIGO Scientific Collaboration) 2015 *Class. Quantum Grav.* **32** 074001
[3] Acernese F *et al* (Virgo Collaboration) 2015 *Class. Quantum Grav.* **32** 024001
[4] Abbott B P *et al* (LIGO Scientific Collaboration and Virgo Collaboration) 2019 *Phys. Rev.* X **9** 031040
[5] Abbott R *et al* (LIGO Scientific Collaboration and Virgo Collaboration) 2021 *Phys. Rev.* X **11** 021053
[6] Abbott R *et al* (LIGO, VIRGO, KAGRA Collaborations) 2021 (arXiv:2111.03606)
[7] Abbott B P *et al* 2016 *Living Rev. Relativ.* **19** 1
[8] Baumgarte T W and Shapiro S L 2021 *Numerical Relativity: Starting From Scratch* (Cambridge: Cambridge University Press)
[9] Pürrer M and Haster C J 2020 *Phys. Rev. Res.* **2** 023151
[10] Ossokine S *et al* 2020 *Phys. Rev.* D **102** 044055

[11] Pratten G *et al* 2021 *Phys. Rev.* D **103** 104056
[12] Estellés H, Colleoni M, García-Quirós C, Husa S, Keitel D, Mateu-Lucena M, Planas M d L and Ramos-Buades A 2021 (arXiv:2105.05872)
[13] Akcay S, Gamba R and Bernuzzi S 2021 *Phys. Rev.* D **103** 024014
[14] Cotesta R, Buonanno A, Bohé A, Taracchini A, Hinder I and Ossokine S 2018 *Phys. Rev.* D **98** 084028
[15] García-Quirós C, Colleoni M, Husa S, Estellés H, Pratten G, Ramos-Buades A, Mateu-Lucena M and Jaume R 2020 *Phys. Rev.* D **102** 064002
[16] Estellés H, Husa S, Colleoni M, Keitel D, Mateu-Lucena M, García-Quirós C, Ramos-Buades A and Borchers A 2020 (arXiv:2012.11923)
[17] Nagar A, Riemenschneider G, Pratten G, Rettegno P and Messina F 2020 *Phys. Rev.* D **102** 024077
[18] Field S E, Galley C R, Hesthaven J S, Kaye J and Tiglio M 2014 *Phys. Rev.* X **4** 031006
[19] Varma V, Field S E, Scheel M A, Blackman J, Gerosa D, Stein L C, Kidder L E and Pfeiffer H P 2019 *Phys. Rev. Res.* **1** 033015
[20] Varma V, Field S E, Scheel M A, Blackman J, Kidder L E and Pfeiffer H P 2019 *Phys. Rev.* D **99** 064045
[21] Blackman J, Field S E, Scheel M A, Galley C R, Ott C D, Boyle M, Kidder L E, Pfeiffer H P and Szilágyi B 2017 *Phys. Rev.* D **96** 024058
[22] Abbott R *et al* (LIGO Scientific, Virgo) 2020 *Phys. Rev. Lett.* **125** 101102
[23] Abbott R *et al* (LIGO Scientific, Virgo) 2020 *Phys. Rev.* D **102** 043015
[24] Varma V, Biscoveanu S, Islam T, Shaik F H, Haster C J, Isi M, Farr W M, Field S E and Vitale S 2022 (arXiv:2201.01302)
[25] Varma V, Biscoveanu S, Isi M, Farr W M and Vitale S 2022 *Phys. Rev. Lett.* **128** 031101
[26] Varma V, Isi M, Biscoveanu S, Farr W M and Vitale S 2022 *Phys. Rev.* D **105** 024045
[27] Varma V, Isi M and Biscoveanu S 2020 *Phys. Rev. Lett.* **124** 101104
[28] Kumar P, Blackman J, Field S E, Scheel M, Galley C R, Boyle M, Kidder L E, Pfeiffer H P, Szilagyi B and Teukolsky S A 2019 *Phys. Rev.* D **99** 124005
[29] Islam T, Field S E, Haster C J and Smith R 2021 *Phys. Rev.* D **103** 104027
[30] Gou L, McClintock J E, Reid M J, Orosz J A, Steiner J F, Narayan R, Xiang J, Remillard R A, Arnaud K A and Davis S W 2011 *Astrophys. J.* **742** 85
[31] Scheel M A, Giesler M, Hemberger D A, Lovelace G, Kuper K, Boyle M, Szilágyi B and Kidder L E 2015 *Class. Quantum Grav.* **32** 105009
[32] Healy J, Lousto C O, Ruchlin I and Zlochower Y 2018 *Phys. Rev.* D **97** 104026
[33] Varma V and Ajith P 2017 *Phys. Rev.* D **96** 124024
[34] Varma V, Ajith P, Husa S, Bustillo J C, Hannam M and Pürrer M 2014 *Phys. Rev.* D **90** 124004
[35] Capano C, Pan Y and Buonanno A 2014 *Phys. Rev.* D **89** 102003
[36] Shaik F H, Lange J, Field S E, O'Shaughnessy R, Varma V, Kidder L E, Pfeiffer H P and Wysocki D 2020 *Phys. Rev.* D **101** 124054
[37] Field S E, Galley C R, Herrmann F, Hesthaven J S, Ochsner E and Tiglio M 2011 *Phys. Rev. Lett.* **106** 221102
[38] Hesthaven J S, Stamm B and Zhang S 2014 *ESAIM: M2AN* **48** 259–83
[39] Blackman J, Field S E, Scheel M A, Galley C R, Hemberger D A, Schmidt P and Smith R 2017 *Phys. Rev.* D **95** 104023
[40] Varma V, Gerosa D, Stein L C, Hébert F and Zhang H 2019 *Phys. Rev. Lett.* **122** 011101
[41] Mroue A H *et al* 2013 *Phys. Rev. Lett.* **111** 241104
[42] Boyle M *et al* 2019 *Class. Quantum Grav.* **36** 195006
[43] Kidder L, *et al* 2021 Spectral Einstein Code (available at: www.black-holes.org/SpEC.html)
[44] York James W J 1999 *Phys. Rev. Lett.* **82** 1350–3
[45] Pfeiffer H P and York J J W 2003 *Phys. Rev.* D **67** 044022
[46] Cook G B and Pfeiffer H P 2004 *Phys. Rev.* D **70** 104016
[47] Lovelace G, Owen R, Pfeiffer H P and Chu T 2008 *Phys. Rev.* D **78** 084017
[48] Lindblom L, Scheel M A, Kidder L E, Owen R and Rinne O 2006 *Class. Quantum Grav.* **23** S447–62
[49] Szilagyi B, Lindblom L and Scheel M A 2009 *Phys. Rev.* D **80** 124010
[50] Rinne O 2006 *Class. Quantum Grav.* **23** 6275–300
[51] Hemberger D A, Scheel M A, Kidder L E, Szilágyi B, Lovelace G, Taylor N W and Teukolsky S A 2013 *Class. Quantum Grav.* **30** 115001
[52] Ossokine S, Kidder L E and Pfeiffer H P 2013 *Phys. Rev.* D **88** 084031

[53] Abbott B P *et al* (The LIGO Scientific Collaboration and the Virgo Collaboration) 2019 *Phys. Rev.* D **100** 104036
[54] Lindblom L, Owen B J and Brown D A 2008 *Phys. Rev.* D **78** 124020
[55] Abbott B P *et al* (LIGO Scientific Collaboration and Virgo Collaboration) 2016 *Phys. Rev. Lett.* **116** 131103
[56] Hild S *et al* 2011 *Class. Quantum Grav.* **28** 094013
[57] Hall E D and Evans M 2019 *Class. Quantum Grav.* **36** 225002
[58] Buonanno A, Kidder L E, Mroue A H, Pfeiffer H P and Taracchini A 2011 *Phys. Rev.* D **83** 104034